



EP/L014106/1

SUPERGEN Wind Hub

Deliverables:

D6.2 Report on structural damage modelling

Delivered by:	University of Strathclyde		
Author(s):	Dr Peyman Amirafshari, Professor Feargal Brennan, Professor Athanasios Kolios		
Delivery date:	01 08 2019		
Distribution list:	Supergen Wind Hub		

Sponsored by:



Table of Contents

List of Figures.....	3
List of Tables	4
Structural Damage Modelling:	5
Introduction	5
Limitations of S-N approach.....	5
Fracture Mechanics Approach.....	7
Crack growth prediction	7
Failure criteria.....	9
Through thickness	9
Failure Assessment diagram	10
Fracture Mechanics framework for structural design.....	12
Damage-tolerant design	13
Inspection reliability (PODs)	14
Inspection strategy.....	15
Design inputs.....	16
Application to a Monopile Offshore Wind Turbine (OWT) support structure.....	17
Case description.....	17
Crack growth in Air	19
Effect of environment	20
Probabilistic Fracture Mechanics.....	21
Target reliability levels	23
Application to a plate failure.....	24
Risk Based design.....	26
Optimising inspection for design	28
Summary.....	29
References	29

List of Figures

Figure 1 Relationship between inspection and design philosophy	6
Figure 2 Crack growth curve diagram	7
Figure 3 Schematic of crack propagation curve according to Paris-Erdogan law (Amirafshari, 2019)	8
Figure 4 Schematic of crack growth models by Paris law	8
Figure 5 Diagram of a surface crack penetrating wall	10
Figure 6 Failure Assessment Diagram (FAD) (Amirafshari, 2019)	12
Figure 7 Fracture Mechanics flow diagram for assessment and design of structures against fatigue failure	13
Figure 8 schematic representation of damage tolerant fracture mechanics approach, adapted from (Anderson, 2005)	14
Figure 9 Relationship between crack size distribution, Probability of detection and detected crack size distribution (Amirafshari, 2019)	14
Figure 10 DNV POD for surface NDE. Replotted from (DNV, 2015)	15
Figure 11 In-service inspection strategies	16
Figure 12 The case study structure diagrams and FEA contour plots for the support structure	18
Figure 13 Failure assessment diagram (FAD) for crack growth in HAZ and in Air environment without inspection	19
Figure 14 Crack growth curves for propagation in HAZ and in Air environment	20
Figure 15 Failure assessment diagram (FAD) for crack growth in HAZ and with free corrosion	20
Figure 16 Crack growth curves for propagation in HAZ and with free corrosion	21
Figure 17 Probabilistic fracture assessment using Monte Carlo method and based on FAD (Amirafshari, 2019)	22
Figure 18 A schematic presentation of the inputs to Probabilistic Fracture Mechanics (Amirafshari, 2019)	22
Figure 19 Example of a time-dependent fatigue and fracture reliability curve	23
Figure 20 Through-thickness Crack geometry diagram	25
Figure 21 Fatigue reliability (FM) of a welded joint in an offshore structure for three different constant amplitude stresses	26
Figure 22 A typical Risk matrix diagram	27
Figure 23 ALARP Carrot diagram based on (HSE, 2001)	28
Figure 24 schematics of Crack growth curves based risk profile	28
Figure 25 Crack growth curves of case study through thickness in a plate considering different first inspection times	29

List of Tables

Table 1 MPI Reliability (BS7910).....	15
Table 2 Design constraints for damage tolerant fracture mechanics design	16
Table 3 Design variables for damage tolerant fracture mechanics design	16
Table 4 Inputs for Fatigue and fracture mechanics assessment	17
Table 5 results for crack growth in HAZ and in Air environment.....	19
Table 6 Examples of target levels of reliabilities specified by standards.....	24
Table 7 Inputs for probabilistic Fatigue and fracture mechanics assessment.....	25

Structural Damage Modelling:

This work package has considered advanced fracture mechanics fatigue damage models to better represent the material and micro-mechanical mechanisms involved in fatigue failure. At present, designers use a relatively crude stress-life approach which does not allow the study of residual stresses, variable amplitude corrosion fatigue effects or surface treatments that are all of vital importance if fatigue resisting offshore structures are to be developed for wind systems. The work package has in particular considered thickness effects, which are unique to monopile structures and are unlike ship and oil & gas structures in having a high degree of structural constraint and therefore unusual fatigue behaviour.

Introduction

Standards such as IEC 61400-3 (IEC, 2009), DNVGL-ST-0126 (DNVGL, 2016 a), DNVGL-ST-0437 (DNVGL, 2016 b) and DNVGL-RP-C203 (DNV, 2010) are commonly used for the design of offshore wind turbines against fatigue failure. Current approaches are solely based on S-N data. Service induced stresses contributing to fatigue damage accumulations are determined from structural analysis and a suitable joint type capable of resisting those stresses for the intended life of the structure are specified.

Fatigue design of steel structures using S-N data is preferred to the Fracture Mechanics approach due to its simplicity. S-N data approach is also considered more reliable since it is based on fatigue test but Fracture Mechanics is based on calculations where additional input variables (e.g. crack growth rate, toughness, and residual stress distributions) need to be considered.

Despite its popularity, a number limitation exists with the S-N data approach with relation to offshore wind turbine structures.

Limitations of S-N approach

Design for inspection: Many structures are designed considering a damage tolerant design philosophy where the structure is expected to tolerate certain levels of fatigue damage until next scheduled inspection (Figure 1). Traditionally, the expected crack size at the time of the inspection is estimated using Fracture Mechanics and a suitable NDT technique capable of detecting the critical crack size is prescribed. In offshore wind turbines, due to access restrictions, the choice of NDT method can be limited to a certain NDT method with a specific detection capability. Therefore, it may be necessary to consider the Probability of Non-Detection (POND) and improve the design for such a scenario. This can only be achieved through a fracture mechanics approach. The S-N approach can only quantify the accumulated damage without providing any information about the size and dimensions of the damage.

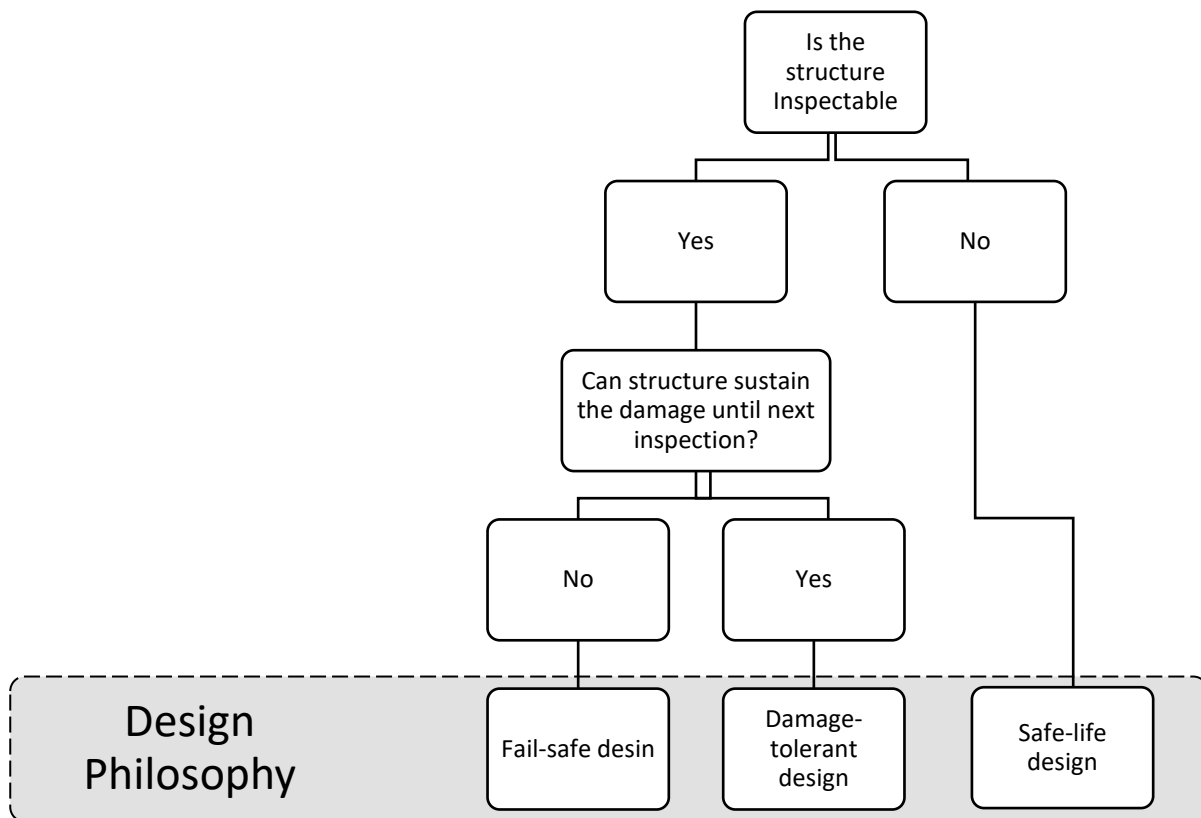


Figure 1 Relationship between inspection and design philosophy

Other limitations:

- **Effect of larger defect sizes:** S-N data is based on the assumption that the initial defect sizes are small, between 0.04 to 0.2 mm, assuming that an appropriate quality control programme is in place during fabrication capable of detecting larger fabrication defects. In practice, reliability and efficiency of such a programme and the NDT techniques are uncertain and vary considerably among fabrication yards. Assessment and design of the welded joints considering the presence of large defects can only be achieved using Fracture Mechanics. An improved joint design using Fracture Mechanics can be achieved allowing for possible fabrication defects left in the structure by, for example, specifying larger thicknesses, higher toughness steels, post weld heat treatment, etc.
- **New welding processes:** There is always efforts to improve structural resistance, fabrication efficiency and weld quality by developing and implementing new welding technologies. Those processes may inevitably have altered characteristics (defect rates, sizes, geometry, residual stresses, toughness, etc.), which affect fatigue failure of the joint. Considering these variables using S-N data will require development of bespoke fatigue test programme (ideally full-scale fatigue testing) which is not always feasible. A more efficient and cost-effective solution is the application of fracture mechanics.
- **New materials:** development and use of new steel grades with higher tensile strength and weld consumable with superior weldability characteristics will inevitably affect fatigue failure of the structure: i.e. higher strength steel will be capable of resisting higher stresses but the toughness properties may not increase leading to shorter fatigue life. Considering such effects is best achieved through a fracture mechanics approach which uses fracture toughness as an input.
- **Shakedown and compressive residual stresses:** Fracture failure of welded joints are directly related to residual stresses. Part of these stresses can be relieved under service or fabrication loads. In pile foundations, since the structure is driven to the soil a considerable amount of

compressive residual stresses are induced into the pile which can potentially improve the fatigue and fracture performance. The effect of compressive residual stress and the shakedown phenomena can be addressed using a fracture mechanics framework.

Fracture Mechanics Approach

Fatigue cracks in welded structures initiate from weld fabrication defects at the joints. Even sound welds often contain small undercuts at the weld toes (Figure 2).

Fracture mechanics approach uses Paris equation to predict crack growth under cyclic stress. The method is based on the assumption that an initial flaw is present at the structure. The initial flaw size depends on the rigour of the fabrication quality control programme. The reliability of the NDT method that is used during the QC programme, the extent of the inspection (100% of partial) and the flaw acceptance criteria will influence such a rigour.

The fracture mechanics enables efficient application of NDT methods for in-service inspection by specifying inspection interval(s) and the most effective NDT which has the capability of reliable detection of the predicted crack size with a required confidence. This is schematised in Figure 2 below, where the NDT inspection (I_1) detects cracks greater than initial flaw size (a_0). If all such cracks are found and repaired the crack growth curve will be shifted down.

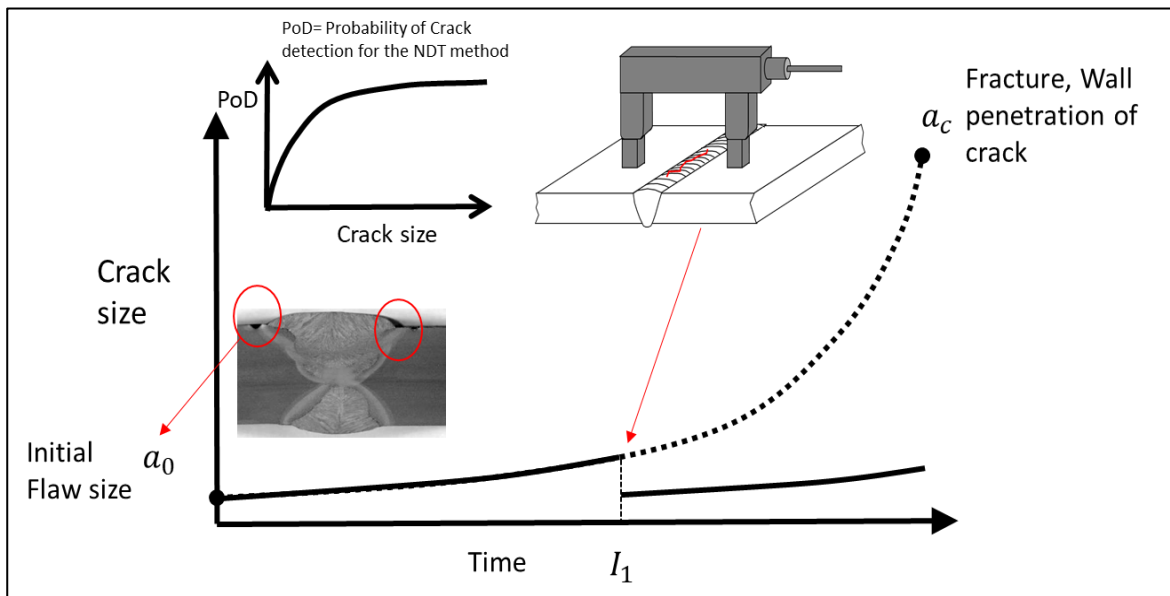


Figure 2 Crack growth curve diagram

Crack growth prediction

Fracture mechanics (FM) enables prediction of crack propagation by using the crack growth rate, schematised in Figure 3. Region A is where crack growth rate occurs as soon as $\Delta K \geq \Delta K_{th}$, where ΔK_{th} is the threshold value of ΔK . The threshold value depends on numerous factors such as the stress ratio = K_{max}/K_{min} , sequence effect, residual stresses, loading frequency, and environment. Region B is where the crack growth rate increases with ΔK to a constant power. Region C is where the crack growth rate increases rapidly until failure occurs as soon as $K \geq K_{critical}$.

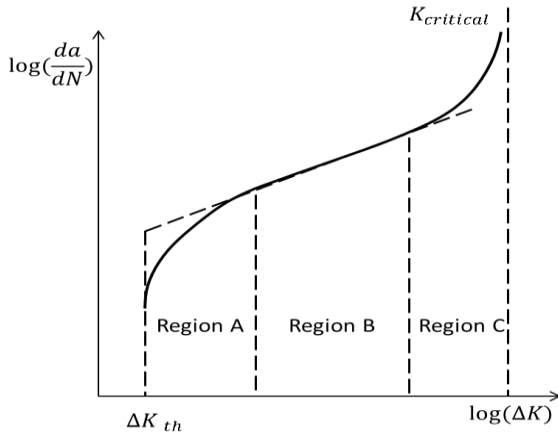


Figure 3 Schematic of crack propagation curve according to Paris-Erdogan law (Amirafshari, 2019)

In the FM approach crack growth rate is commonly described by the Paris-Erdogan equation:

$$\frac{da}{dN} = C * \Delta K^m \quad (1)$$

where, $\frac{da}{dN}$ is the rate of crack growth with respect to load cycles, ΔK is the change in stress intensity factor, and C and m are material constants. Recently a bilinear crack growth model has been used, as well (Figure 4). (BS7910, 2015) recommended model is the bilinear model, while the simplified model is cited, as well.

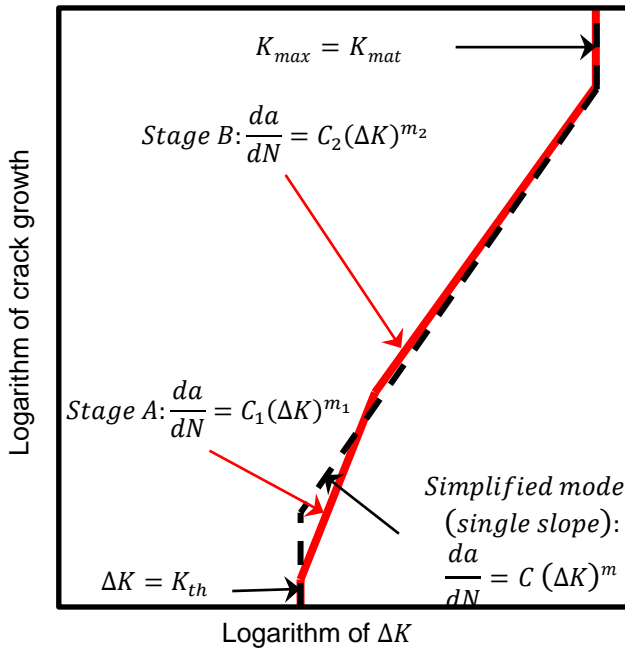


Figure 4 Schematic of crack growth models by Paris law

Stress intensity factor is described by:

$$\Delta K = Y\sigma\sqrt{\pi a} \quad (2)$$

where, a is flaw size, σ is stress at the flaw, and Y is the geometry function which depends on both the geometry under consideration and the loading mode. There are several ways in which solutions for Y can be obtained. Although it is possible to derive solutions for simple geometries

analytically, e.g. using ‘weight functions’, numerical techniques are more commonly used (finite elements, finite difference or boundary elements methods).

In practice critical a_f is calculated by substituting K_{mat} , material fracture toughness, in equation (2); $K_{mat} = Y\sigma\sqrt{\pi a}$, then (provided Y is a constant for all crack sizes) using equation (3) number of cycles to failure can be calculated.

$$N = \int_{a_0}^{a_f} \frac{da}{C(\Delta K)^m} = \frac{1}{A * Y^m * \Delta \sigma^m * \pi^{\frac{m}{2}}} * \frac{a_f^{(1-\frac{m}{2})} - a_0^{(1-\frac{m}{2})}}{1 - \frac{m}{2}} \quad (3)$$

Time-dependent crack size can be calculated by rearranging equation (3):

$$a = \left(\frac{m-2}{2} \right) \sqrt{N * \left(\left(A * Y^m * \Delta \sigma^m * \pi^{\frac{m}{2}} \right) * \left(1 - \frac{m}{2} \right) \right) + a_0^{(1-\frac{m}{2})}} \quad (4)$$

Offshore structure are not subjected to constant amplitude stress, but a variable amplitude stress spectrum. If the long-term stress distribution is converted into a step function of n blocks generally of equal length in $\log N$, the crack size increment for the step i is:

$$\Delta a_i = C(\Delta K_i)^m \Delta N_i \quad (5)$$

moreover, the final crack size at the end of the N cycles is obtained by summing equation for the n stress blocks:

$$a_N = a_0 + \sum_{i=1}^N \Delta a_i \quad (6)$$

Equation (5) is only valid for small values of Δa_i since ΔK_i depends on the crack size, which requires dividing the stress range spectrum into a large number of stress blocks.

The number of cycles to failure may, alternatively, be calculated according to equation (7) using an equivalent constant amplitude stress ranges $\Delta \sigma_{eq}$ giving the same amount of damage (Naess, 1985):

$$\Delta \sigma_{eq} = \left[\int_0^\infty \Delta \sigma^\beta p_{\Delta \sigma}(\Delta \sigma) d\Delta \sigma \right]^{1/\beta} \quad (7)$$

where β is the contribution factor. For the central part of the crack growth curve β is often about 3.0. $p_{\Delta \sigma}(\Delta \sigma)$ is the probability density function of stress range $\Delta \sigma$.

Failure criteria

Through thickness

A commonly chosen failure criteria for fatigue crack growth assessment is the through-thickness criteria. The initial fatigue crack is assumed to be a surface breaking flaw growing along the height (a) and length ($2C$) of the flaw. The failure happens when the crack height penetrates through the thickness of the wall (Figure 5).

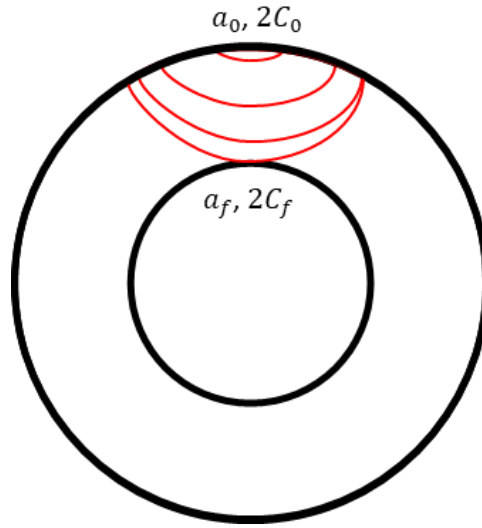


Figure 5 Diagram of a surface crack penetrating wall

There are, however, two major shortcoming for this criteria:

1. The structure may still be able to sustain the through-thickness crack until the crack length reaches a critical length. This is particularly common in thin wide plates.
2. In through thickness failure criteria the crack grows under cyclic loading which corresponds to normal service loading until it becomes through thickness. In reality, failure often happens during extreme load occurrences. The cracked structure may fail under such extreme loading.

To address above limitation the failure assessment diagram (FAD) may be adopted. The approach can assess the failure of the through-thickness crack as well as implementing extreme load occurrences by treating them as the primary stress. The approach is explained below.

Failure Assessment diagram

When a crack propagates through a structure, ultimately the crack size reaches a critical size a_f . a_f corresponds to a critical stress intensity factor, usually taken as characteristic of the fracture toughness K_{mat} , at which fracture happens. Alternatively, if the applied load is high and structure tensile strength is low, the structure may reach its tensile strength capacity and fail by plastic collapse. The latter is more favourable as it is usually associated with large deformations prior to failure providing some level of warning. In between brittle fracture and global collapse is an elastoplastic failure mode, where failure occurs before reaching the plastic capacity or toughness limit; this has been best described by failure assessment diagram (FAD) in the R6 procedure in 1976 and improved over time by e.g. including the options available to model specific material properties. The body of knowledge encapsulated in R6 affected the development of British Standards documents in various ways over the years, leading to BS7910:1999 (Yates, 2010) and the latest version at the time of writing, (BS7910, 2015).

The failure assessment line (FAL) represents the normalised crack driving force:

$$K_r = \frac{K_{elastic}}{K_{elastic\ plastic}} \quad (8)$$

K_r is equal to 1 where applied load is zero and declines as the ratio between applied load and yield load (L_r) increases towards collapse load (see Figure 6).

The plastic collapse load is calculated based on yield stress. However, the material has further load carrying capacity as it work-hardens through yield to the ultimate tensile stress. To take this into account the rightwards limit of the curve is fixed at the ratio of the flow stress to the yield stress:

$$L_r = \frac{\sigma_{flow}}{\sigma_Y} \quad (9)$$

The flow stress is the average of the yield and ultimate stresses:

$$\sigma_{flow} = \frac{\sigma_Y + \sigma_U}{2} \quad (10)$$

If the assessment point lies inside the envelope (below the FAL), the fracture mechanics driving parameter is lower than the materials resistance parameter and the part should be safe, otherwise there is a risk of failure. The failure assessment diagram can be determined with one of the procedures provided by (BS7910, 2015). As it is illustrated in Figure 6, FAD may be categorised into three different zones: Zone 1 is the fracture dominant zone, Zone 2 is the elastoplastic region or the knee region, and Zone three is the collapse dominant zone.

(BS7910, 2015) has three alternative approaches Option 1, Option 2 and Option 3. These are of increasing complexity in terms of the required material and stress analysis data but provide results of increasing accuracy.

Option 1 (BS7910, 2015) is a conservative procedure that is relatively simple to employ and does not require detailed stress/strain data for the materials being analysed. The Failure Assessment Line (FAL) for the Option 1 analysis is given by:

$$K_r = f(L_r) = (1 + 0.5 * L_r^2)^{-0.5} * (0.3 + 0.7 * \exp(-\mu * L_r^6)) \quad (11)$$

for $L_r < 1$, where: $\mu = \min \left[0.001 \frac{E}{\sigma_Y}; 0.6 \right]$.

and:

$$K_r = f(L_r) = f(1) L_r^{(N-1)/2N} \quad (12)$$

For, $1 < L_r < L_{r,max}$, where N is the estimate of strain hardening exponent given by: $N = 0.3(1 - \frac{\sigma_Y}{\sigma_{UTS}})$. and $L_{r,max} = \frac{\sigma_{flow}}{\sigma_Y}$.

Option 2A/3A of BS 7910:2005 generalised FAD, is similar but not identical to Option 1 (BS7910, 2015).

$$K_r = (1 - 0.14 * L_r^2) * (0.3 + 0.7 * \exp(-0.65 * L_r^6)) \quad (13)$$

The (BS7910, 2015) Option 2 FAD is based on the use of a material-specific stress-strain curve. The assessment line can be written as:

$$K_r = f(L_r) = \left[\frac{E \varepsilon_{ref}}{L_r \sigma_Y}, \frac{L_r^3 \sigma_Y}{2E \varepsilon_{ref}} \right]^{-0.5} \quad (14)$$

ε_{ref} is the true strain obtained from the uniaxial tensile stress-strain curve at a true stress $L_r \sigma_Y$. (BS7910, 2015).

The option 3 failure assessment curve is specific to a particular material, geometry and loading type using both elastic and elastic-plastic analyses of the flawed structure. It is given by:

$$f(L_r) = \sqrt{\frac{J_e}{J}}, \text{ for } L_r < L_{max} \quad (15)$$

$$f(L_r) = 0, \text{ for } L_r > L_{max} \quad (16)$$

J_e is the value from the J-integral from the elastic analysis at the load corresponding to the value L_r . The Option 3 curve is not suitable for general use. It is useful only for specific cases as an alternative approach to Options 1 and 2 (BS7910, 2015).

Options 1&2 (BS7910, 2015) and Option 2A/3A (BS7910:2005) for structural steel with tensile stress of 550 MPa and Yield stress of 450 MPa are illustrated in Figure 6. It can be seen that the greatest difference between the three plotted locus is in the collapse region.

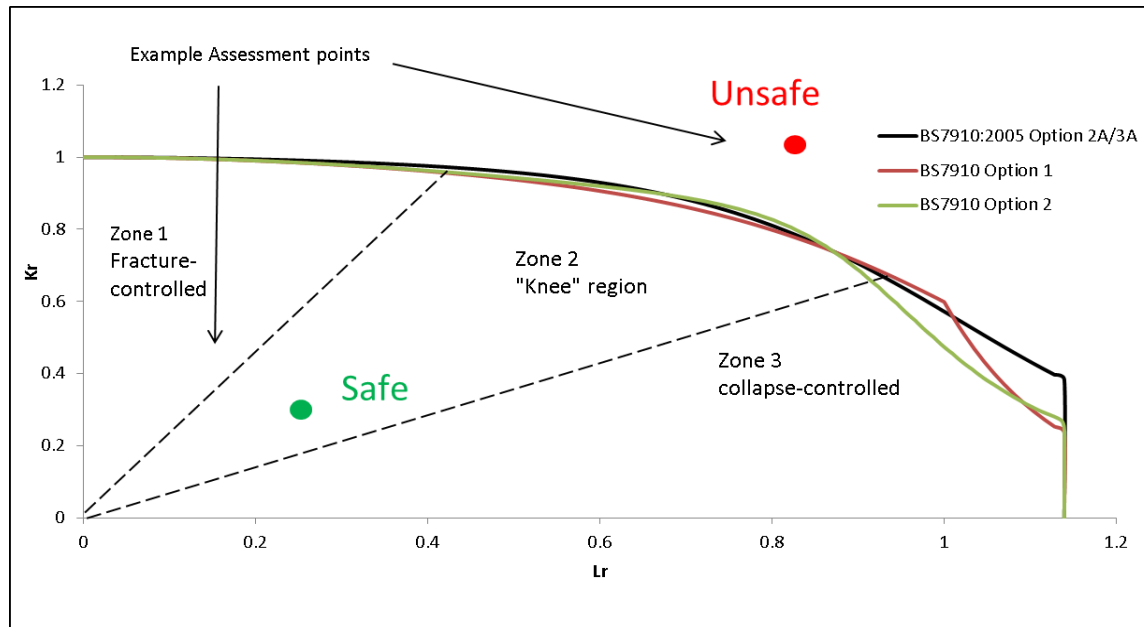


Figure 6 Failure Assessment Diagram (FAD) (Amirafshari, 2019)

Fracture Mechanics framework for structural design

The general design procedure in structural engineering is to design the structure based on the ultimate limit state (ULS) and check or improve the design to fulfil other relevant limit states such as serviceability limit state (SLS) or fatigue limit state (FLS). The fracture mechanics approach can be used to improve structural design. As illustrated in Figure 7, after determining required inputs, such as structural dimensions (determined by structural design based on ULS), initial flaw size, material toughness and tensile properties, stress at the flaw, and parameters of Paris equation, the increased crack size for an increment of time (number of cycles) can be estimated. The predicted crack size is then compared against failure criteria. The procedure is repeated for the next time increment until the failure. If the failure is predicted to occur before intended life of the structure the fatigue life may be enhanced by changing variables that affect the fatigue failure such as structural dimensions, quality control requirements (initial flaw

size), post fabrication improvements (e.g. post weld heat treatment), or by specifying inspection interval(s).

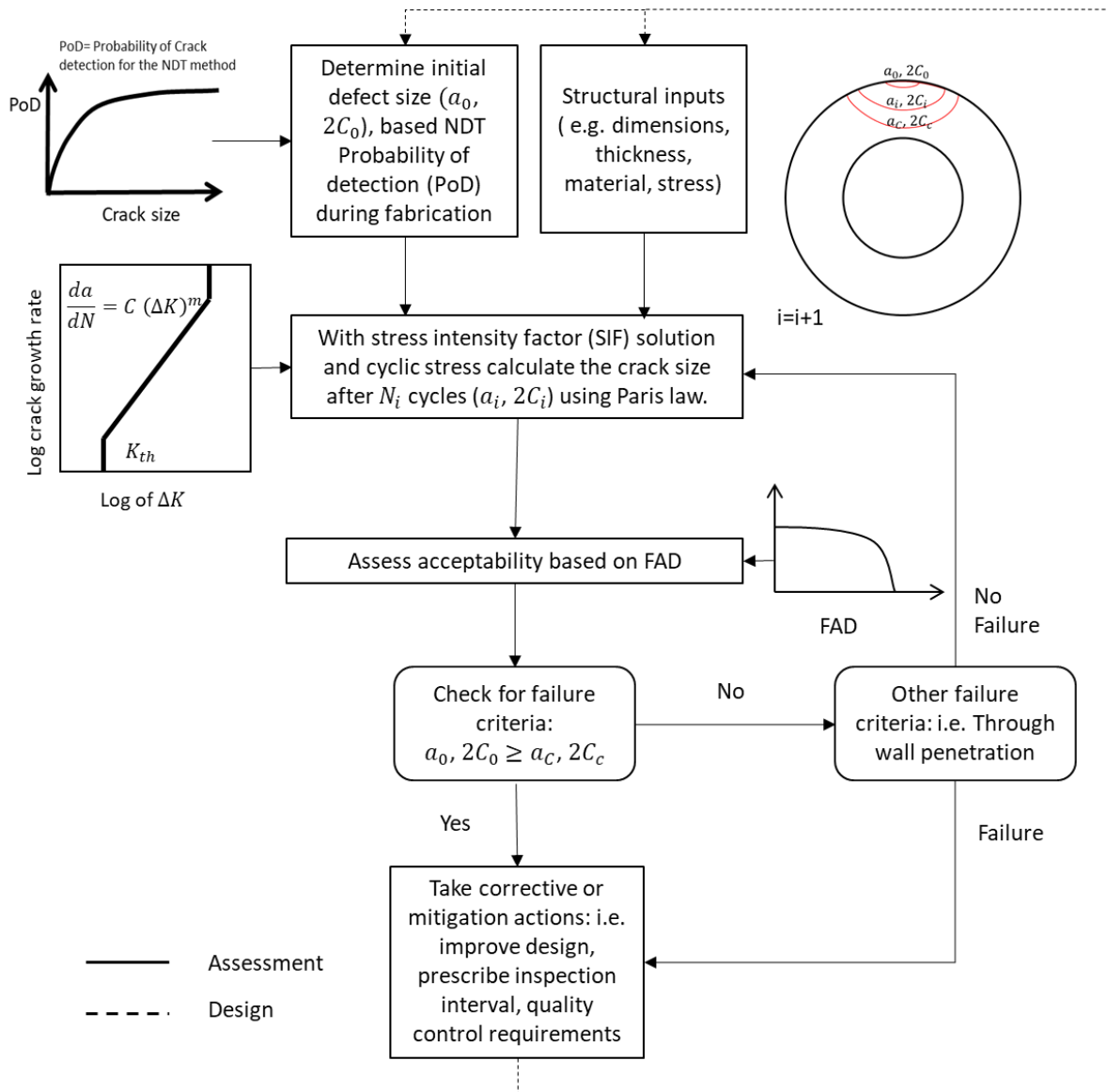


Figure 7 Fracture Mechanics flow diagram for assessment and design of structures against fatigue failure

Damage-tolerant design

The term damage-tolerance fracture mechanics normally refers to a design methodology in which fracture mechanics analyses predict remaining life, and specify inspection intervals. This approach is typically applied to structures prone to time dependent crack growth. The damage tolerance philosophy allows flaws to remain in the structure, provided they are well below the critical size.

Once the critical crack size has been estimated, a safety factor is applied to determine the tolerable flaw size a_t . The safety factor should be based on uncertainties in the input parameters (e.g. stress, parameters in the Paris equation and toughness). Another consideration in specifying the tolerable flaw size is the crack growth rate; a_t should be chosen such that da/dt at this flaw size is relatively small, and a reasonable length of time is required to grow the flaw from a_t to a_c (Anderson, 2005). This is shown schematically in Figure 8.

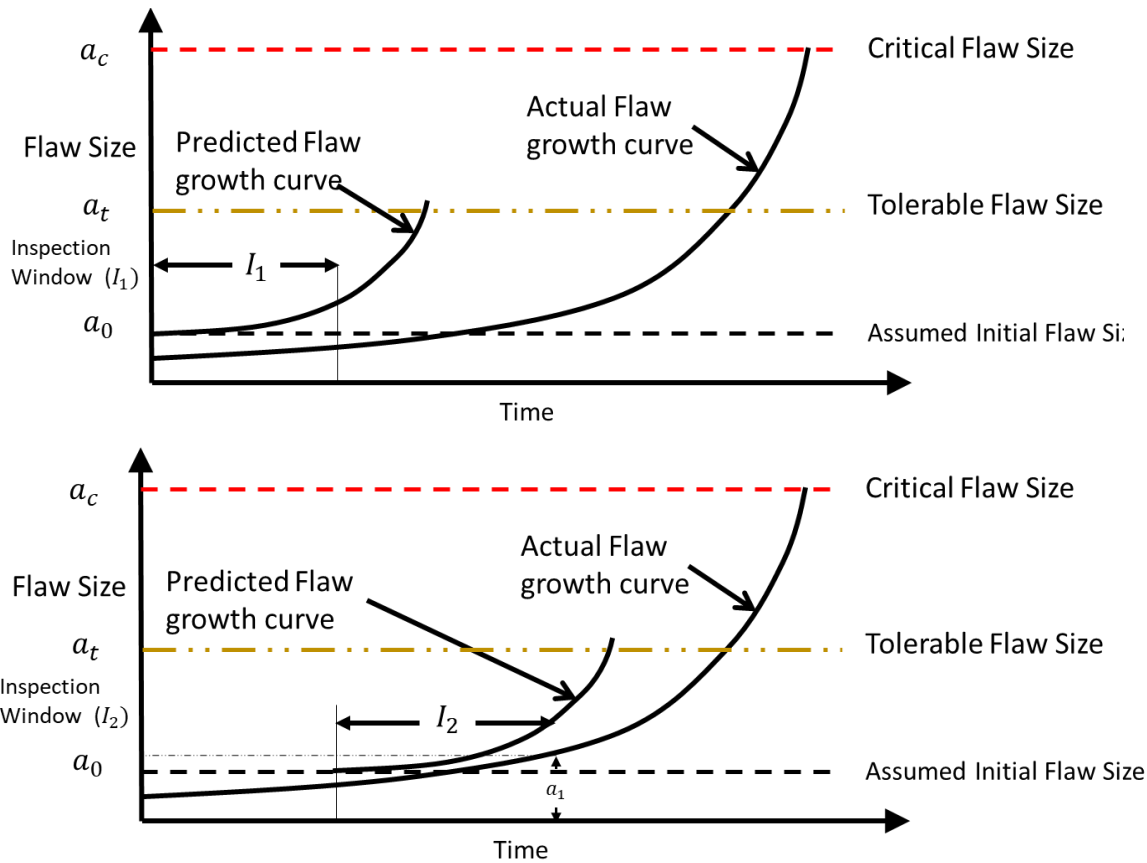


Figure 8 schematic representation of damage tolerant fracture mechanics approach, adapted from (Anderson, 2005)

Inspection reliability (PODs)

NDE methods can only detect a limited number of defects of a certain size. For instance, an NDE method with 50% probability of detection at a certain size, is expected to miss 50% of the defects of that size, in other words, the real number of the defects with that size is likely to be 100% more than detected. In structural integrity assessment, it is often convenient to plot detection probability against defect size, which constructs the so-called probability of detection curve (Figure 10). Detection capabilities of non-destructive examination methods is directly related to sizing of flaws. The bigger the flaw sizes the more likely that they are detected. Figure 9 shows the relationship between detected defect size distribution, the probability of detection of defect sizes and the actual defect size distribution that are present in the structure.

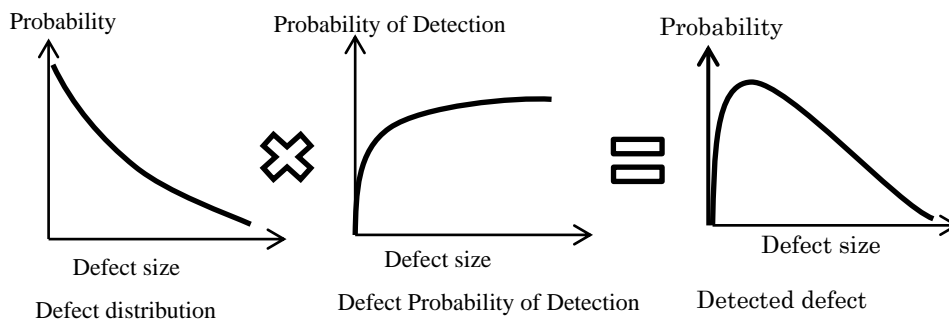


Figure 9 Relationship between crack size distribution, Probability of detection and detected crack size distribution (Amirafshari, 2019)

PoDs for NDT methods are highly dependent on various factors such as, the operator skills, testing environment, test specimen (thickness, geometry, material, etc.), type of the flaw,

orientation and location of the flaw. Hence, accurate estimation of PoD curves requires individual PoD test programmes for specific projects. However, a number of lower bound generic models are available in the literature for some specific NDT methods. Two of such models, that are relevant to this work, are given in Figure 10 and Table 1 below.

Further information about derivation, application and limitations of PoD can found in (Georgiou, 2006).

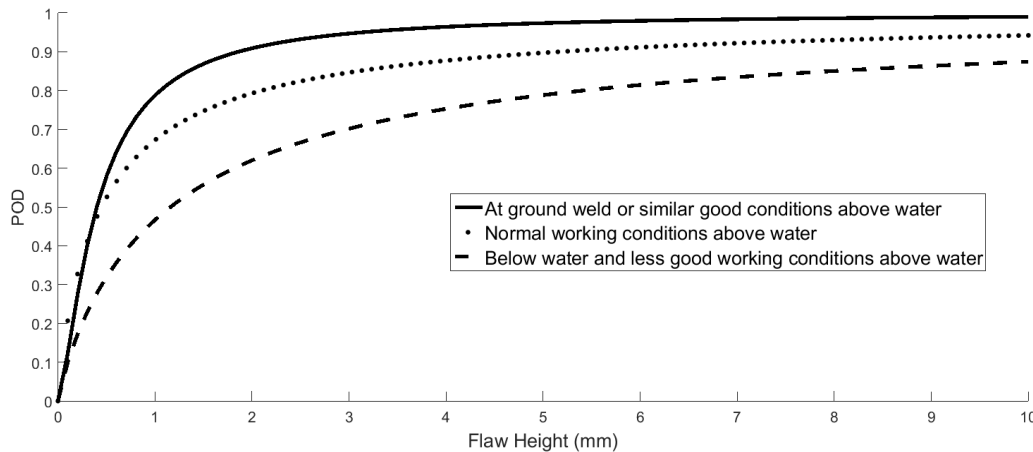


Figure 10 DNV POD for surface NDE. Replotted from (DNV, 2015)

Condition		Flaw Length mm	Flaw through- thickness mm	Length sizing accuracy mm
Machined or ground		5	1.5	±2
As welded:	With local dressing	10	2	±5
	With poor profile	20	4	±10

Table 1 MPI Reliability (BS7910)

Inspection strategy

Fracture mechanics analysis is closely tied to inspection method. The inspection method provides input to the fracture analysis, which in turn helps to define inspection intervals. A structure is inspected at the beginning of its life as a quality control measure. If no significant flaws are detected, the initial flaw size is set at an assumed value a_0 , which corresponds to the largest flaw that might be missed by NDE.

Generally, there are two strategies in section of structures that are susceptible to damage mechanisms (Figure 11):

1. The inspection schedules are fixed: In this case the fracture mechanics can be used to design the structure so that the possible cracks remain below tolerable limits and to predict the crack size in order to select an appropriate NDT method.
2. Inspection schedule is not fixed: In this case, the inspection interval and the NDT method can be optimised in such a way that the inspection results in a safer condition or a minimised cost of maintenance and failure.

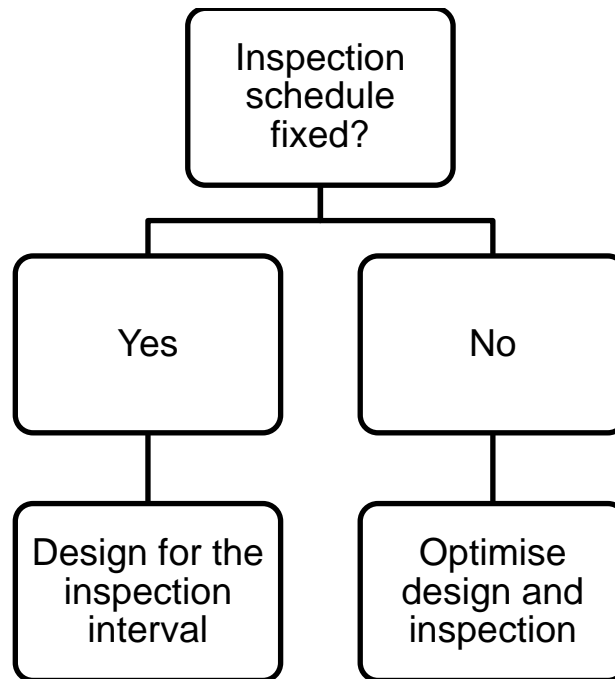


Figure 11 In-service inspection strategies

Design inputs

Damage tolerant Structural design based in fracture mechanics involves various inputs that are related to through-life management of the structure as we as traditional structural design parameters. The key input for damage tolerant fracture mechanics design are listed in Table 2 and Table 3 below.

Design constraints		
Inspection Capabilities		Target reliabilities
Available NDT methods		Cost analysis (i.e. Repair costs, loss of service)
Cost of inspection		Target values defined by standards
NDT reliabilities (POD)		Intended by S-N based method

Table 2 Design constraints for damage tolerant fracture mechanics design

Design variables		
Inspection and Monitoring options:		Design options
NDT methods		Structural design options <ul style="list-style-type: none"> • Thickness • Redundancy • Material selection
Condition monitoring		Fabrication specifications: <ul style="list-style-type: none"> • Weld profile improvements • Post Weld Heat Treatment • Quality Control(i.e. NDT during fabrication, Tolerance limits)

Table 3 Design variables for damage tolerant fracture mechanics design

Application to a Monopile Offshore Wind Turbine (OWT) support structure

Application of fatigue design based on fracture mechanics to a baseline NREL 5MW offshore wind turbine (OWT) supported on a monopile structure (Figure 12) is demonstrated here. Further information about the structure and the Finite Element Analysis can be found in (Gentils et al., 2017).

Case description

Case Description		
Structure	NREL 5MW OWT	
Material Properties	Young Modulus	210
	Poisson Ratio	0.38
	Yield stress	355
	Tensile strength	550
	Toughness	200 MPa* m ^{0.5} assumed
Fatigue assumptions	Crack growth model	Single slope Crack growth
	Cyclic stress	Equivalent constant amplitude stress 51.2 MPa
	Stress Intensity Solution	Surface flaw in a Plate
	Paris Law Constants	$m = 3.9$, $C = 3.814 * 10^{-16}$ for Crack growing in HAZ and in Air, $m = 3.3$, $C = 4.387 * 10^{-14}$ for Crack in HAZ and in with free corrosion, (for da/dN in mm/cycle, and ΔK , in $N/mm^{0.5}$), (Mehmanparast et al., 2017)
	Design cycles in life	$N_{life} = \eta_a * \eta_{rated} * (20 [year] * 365 [day per year] * [hour per year] * 60 [min per hour])$, for this structure = $1.253 * 10^8$
Fracture assumptions	FAD	BS 7910 Option 1
	Primary stress	209 MPa
	Secondary stress	Weld Residual stress= 100 MPa, assumed
	Thickness (B)	60 (mm)
	Initial Flaw dimensions (a*2C)	(1.5 mm * 5 mm)

Table 4 Inputs for Fatigue and fracture mechanics assessment

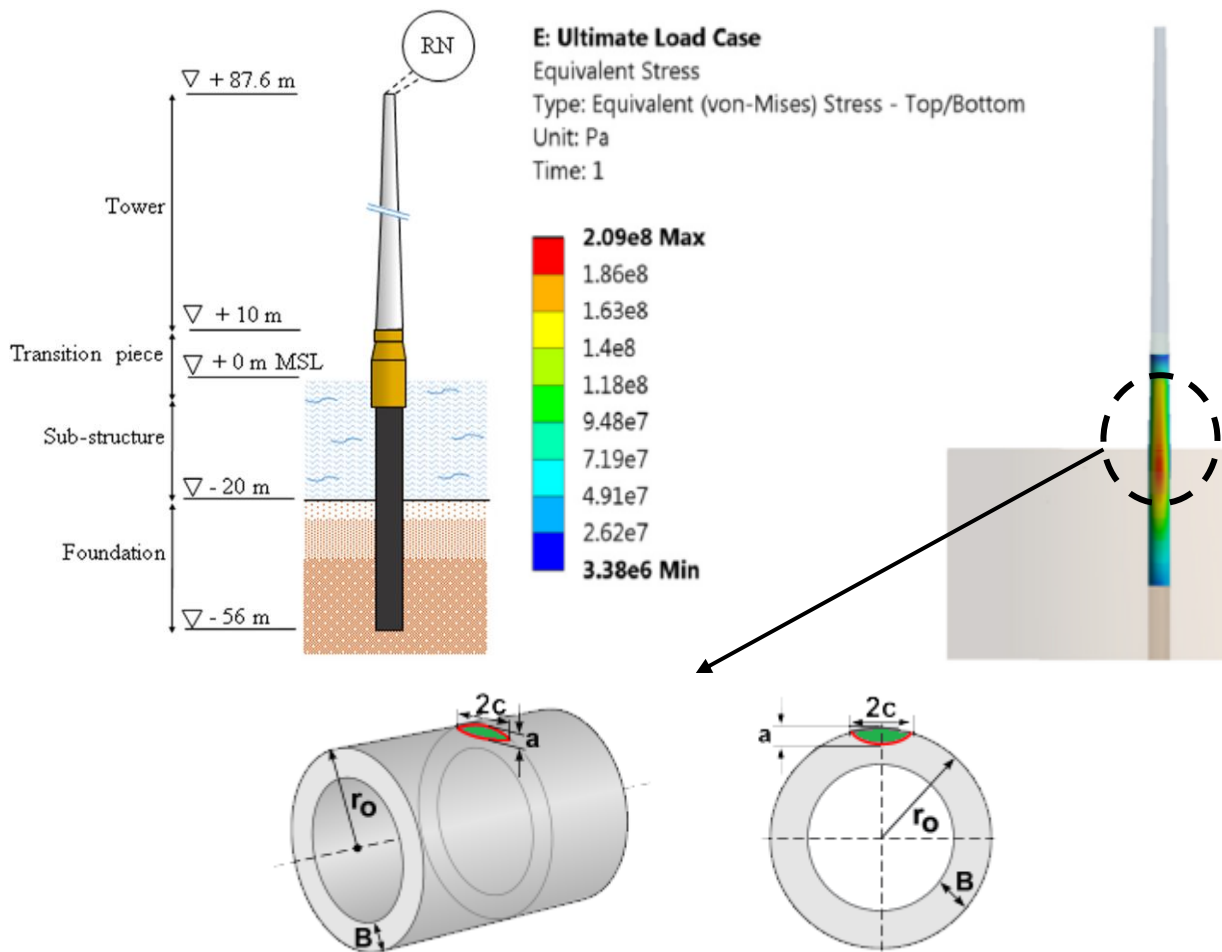


Figure 12 The case study structure diagrams and FEA contour plots for the support structure

Fatigue cracks normally initiate from small toe undercut weld defects (Figure 2), thus, in this study a semi-spherical flaw growing in heat affected zone (HAZ) of the joint is assumed. NDT inspection techniques are used during fabrication as part of quality control scheme. Magnetic particle inspection (MPI) is an effective, and commonly used method to detect surface breaking flaws. Here, initial flaw size is conservatively assumed to be equal to 90 % PoD of MPI method for ground flushed welds (Table 1). Primary fracture stress is taken as caused by ultimate limit state (ULS) design stress (Figure 12) corresponding to the parked wind turbine, under the 50-years Extreme Wind Model (EWM) with the 50-years Reduced Wave Height (RWH) and Extreme Current Model (ECM), defined as the Design Load Case (DLC) 6.1b and 2.1 for (IEC, 2019) and (DNV, 2013) standards, respectively. Load safety factors of 1.1 and 1.35 are applied on the gravitational load and other loads (i.e. wind, wave and current loads), respectively. The crack growth stress is taken as the fatigue load case corresponds to an operating state under Normal Turbulence Model (NTM) and Normal Sea State (NSS) where wave height and cross zero periods are obtained from the joint probability function of the site, assuming no current; it corresponds to the DLC 1.2 from the IEC standard (IEC, 2019) and is assumed to represent the entire fatigue state. Load safety factor for fatigue is equal to 1.0, according to the IEC standard (Gentils et al., 2017). Paris law parameters reported by (Mehmanparast et al., 2017) for offshore wind monopole weldments has been adopted. Other key assumptions and inputs for fatigue and fracture mechanics assessment are given in Table 4.

Crack growth in Air

Crack growth parameters in Paris equation for ferritic steels depend on the, cyclic stress ratio, and environmental condition (Amirafshari and Stacey, 2019). In presence of effective corrosion protection measures, in air conditions apply. The design goal is to design the structure for fatigue under such a condition and provide sufficient corrosion protections through appropriate fabrication practices and through life inspection.

Fatigue and fracture results for cracks propagation in air environment are given in Table 5. Tolerable crack sizes need to be selected way below critical sizes by considering some level of safety factors. As described earlier, the chosen tolerable crack size needs to be determined in a region of crack size where crack growth rate with respect to time is small to allow for a long time before failure but large enough to be detected by the in-service inspection technique. Here, tolerable crack height of 5.2 mm is chosen which gives 70 to 90 percent Probability of Detection (PoD) depending on the inspection condition (Figure 10). As shown in Figure 13, this will provide a good safety factor and at least 6 years before failure (Figure 14).

Assessment results		
Critical Crack size	$a_c = 45 \text{ mm}$	$2C_c = 116 \text{ mm}$
Tolerable crack size (Assumed)	$a_t = 5.2 \text{ mm}$	$2C_t = 12 \text{ mm}$
	$Lr_t = 0.592$	$Kr_t = 0.128$

Table 5 results for crack growth in HAZ and in Air environment

Figure 10 shows assessment points from initial crack propagation at start of service life to the final year of service. If the service life continues the structure is likely to fail in elasto-plastic mode.

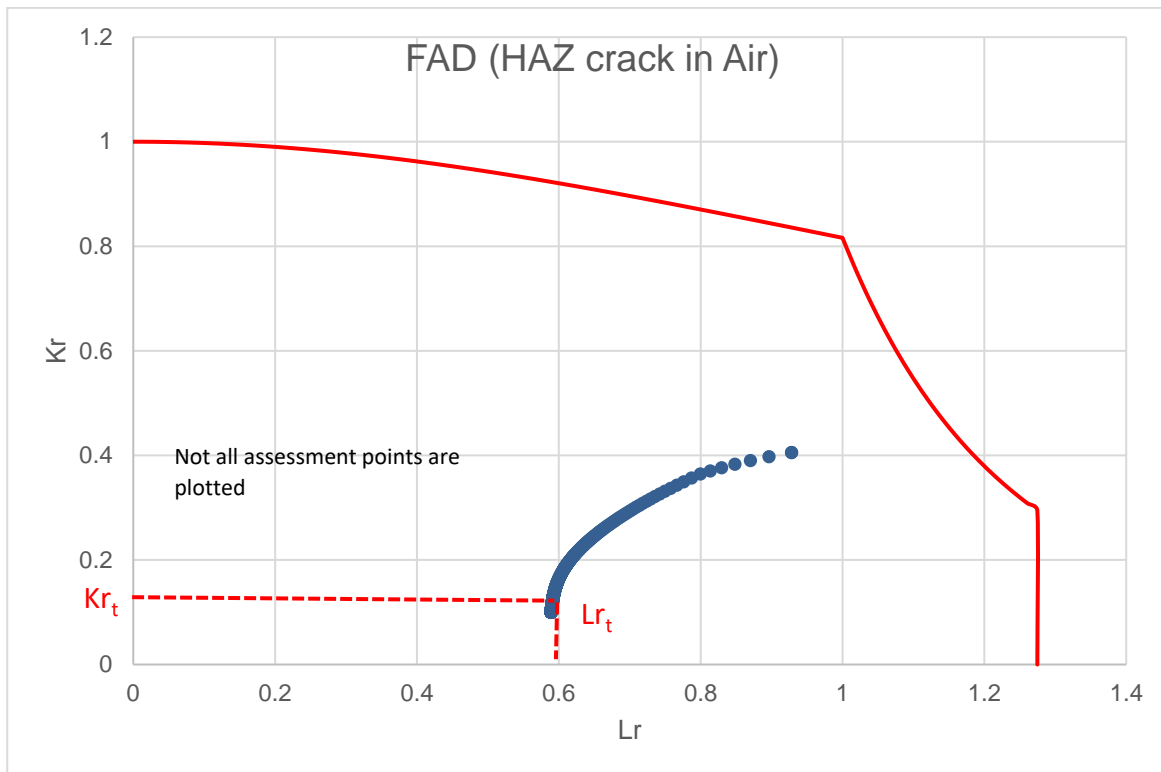


Figure 13 Failure assessment diagram (FAD) for crack growth in HAZ and in Air environment without inspection

As explained earlier a damaged tolerant design is closely tied to in-service inspection. Assuming an inspection at year 12 of service will reduce the predicted crack size to initial crack size

assuming that no crack is detected or repaired if detected. This is shown with solid lines after year 12 in Figure 14. The final year crack size will remain below the tolerable limits.

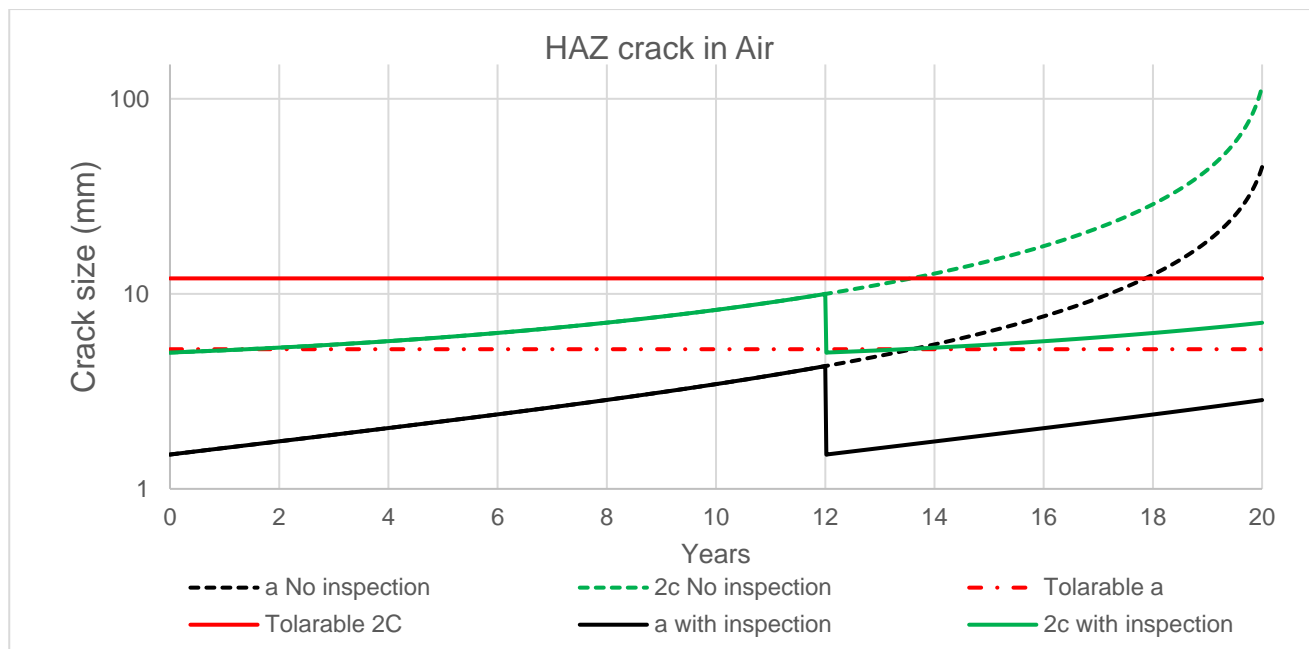


Figure 14 Crack growth curves for propagation in HAZ and in Air environment

Effect of environment

In the event of insufficient corrosion protection, the fatigue crack growth will be accelerated. The accelerated crack growth rate is reflected in fracture mechanics through changing Paris law constants to those observed in corrosive environment. This is shown in Figure 15 and Figure 16, where the previously studied defect is assessed under free corrosion environment instead of the air environment. It is observed that failure is predicted to occur as early as 3.4 years after commissioning. One strategy could be an increased attention to execution of corrosion protection measures prior to commissioning. Additionally the joint should be inspected for the signs of corrosion at least every three years.

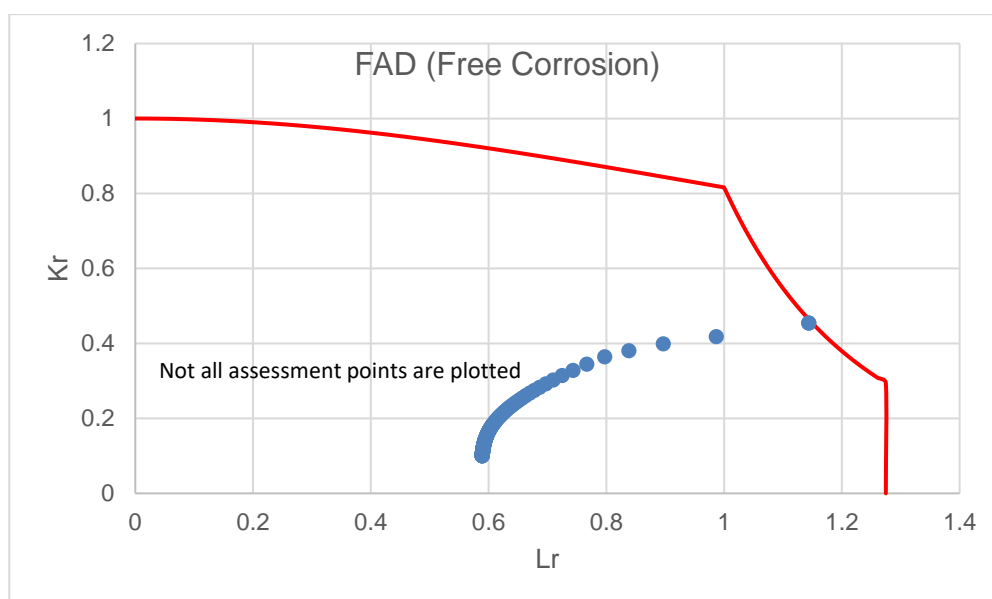


Figure 15 Failure assessment diagram (FAD) for crack growth in HAZ and with free corrosion

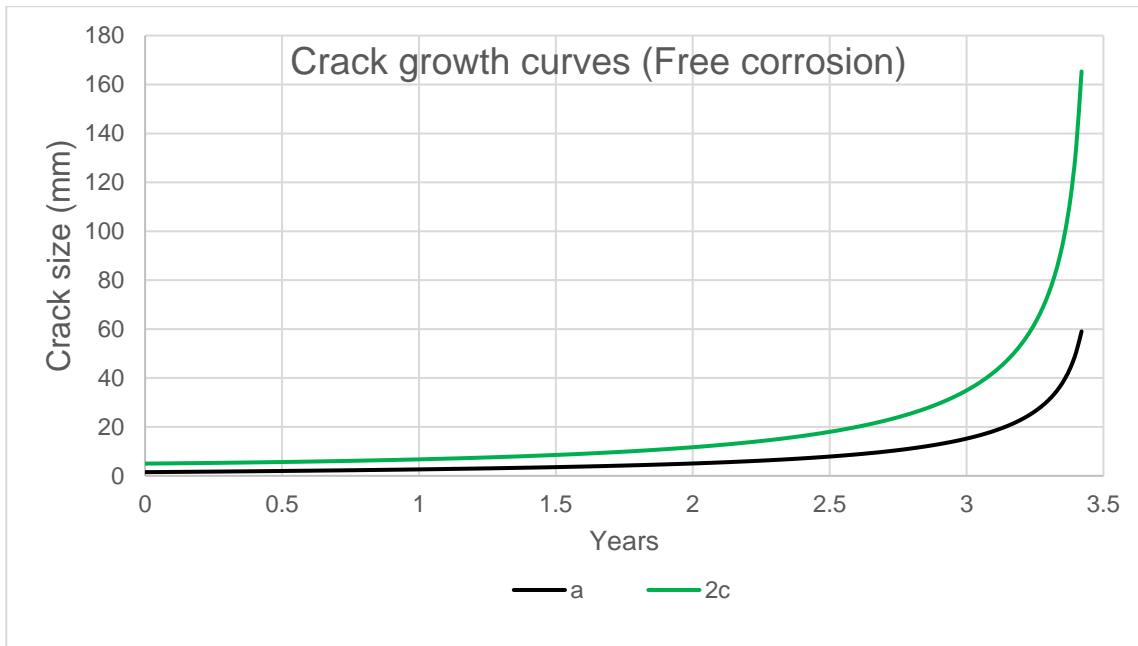


Figure 16 Crack growth curves for propagation in HAZ and with free corrosion

Probabilistic Fracture Mechanics

Fracture mechanics approaches are commonly used deterministically and generally have a hierarchical nature, i.e. the analyst may progressively reduce conservative assumptions by increasing the complexity level of the analysis and consequently the precision of results until the operation of the structure is found to be fit-for-service. Otherwise, the structure will require a repair, a reduction of service (for example lowering primary stress) or resistance improvements (i.e. reduction of secondary stresses by stress relief techniques). This type of approach is particularly useful in the assessment of safety cases where the aim is to demonstrate that the structure is safe given conservative assumption of input variables.

In deterministic analyses uncertainty in variables are dealt with by taking upper bound and lower bound of those variables- upper bound values of applied variables such as stress and flaw size, with lower bound values of resistance variables such as fracture toughness. In reality, the probability of all unfavourable conditions occurring at the same time is very low and often too conservative. An alternative approach is a probabilistic analysis, in which, uncertain variables are treated stochastically and as random variables.

In probabilistic assessments, all possible combinations of input variables leading to failure are compared against total possible combinations, and a probability of failure is estimated instead of a definite fail or not-fail evaluation. Probabilistic analysis is also in-line with the damage tolerant strategy. The failure probability for the limit state function may be estimated using one of available analytical, numerical or simulation methods such Monte Carlo simulation. Figure 17 shows Probabilistic fracture assessment using Monte Carlo method and based on the FAD.

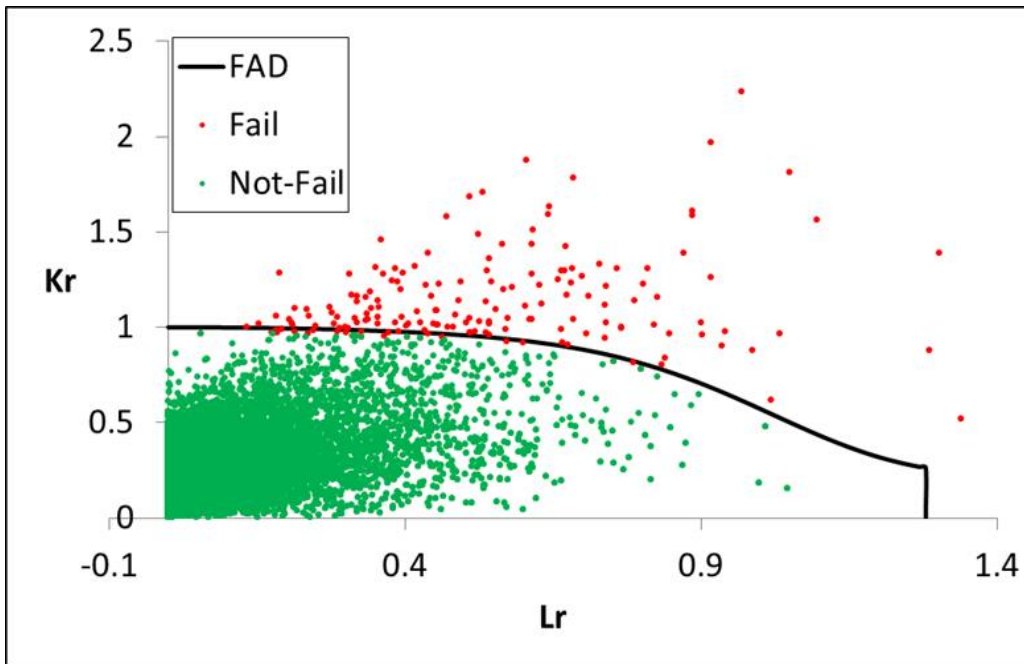


Figure 17 Probabilistic fracture assessment using Monte Carlo method and based on FAD (Amirafshari, 2019)

One limitation of deterministic fracture mechanics is that conservative prediction of critical defect size and the time to the failure may reduce inspection efficiency by targeting wrong defect sizes and at a wrong time in service, whereas probabilistic assessment will provide a more efficient result (Lotsberg et al., 2016). Probabilistic failure assessment of the structures is also known as Reliability analysis. These two terminologies are often used interchangeably.

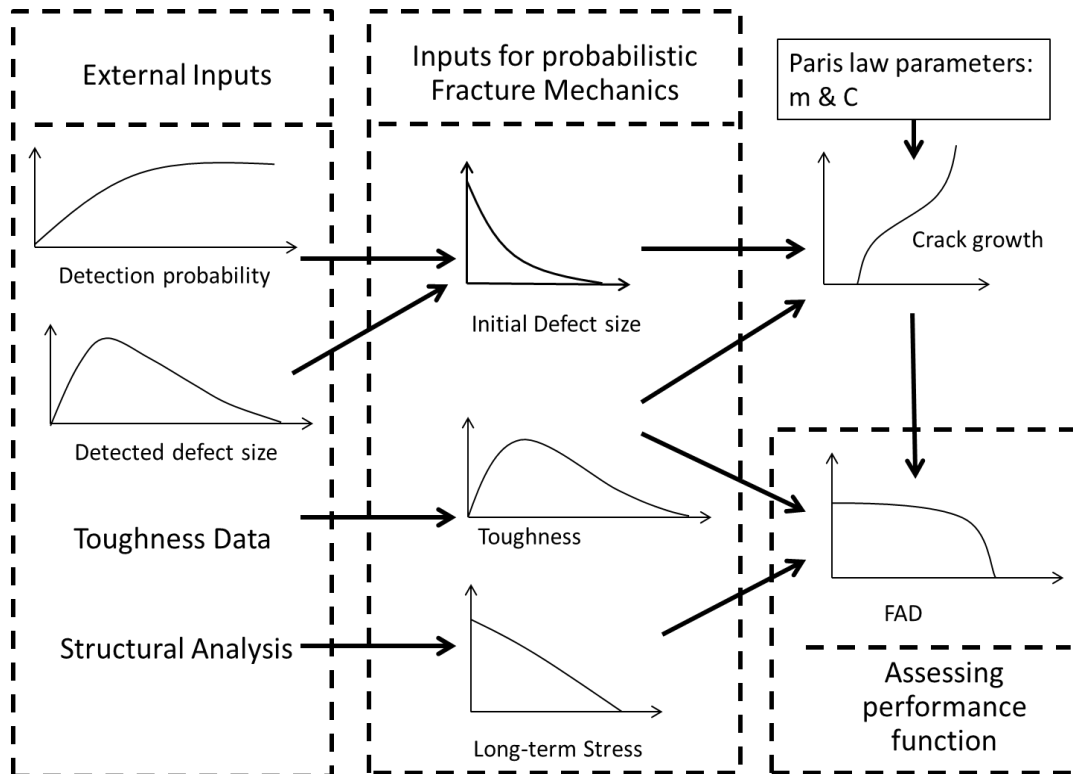


Figure 18 A schematic presentation of the inputs to Probabilistic Fracture Mechanics (Amirafshari, 2019)

Figure 18 shows schematic presentation of the inputs to probabilistic fracture mechanics. Probabilistic fatigue and fracture analysis will predict the time-dependent failure probability of

the structure (Figure 19). The predicted reliability will then need to be compared against an appropriate target reliability level.

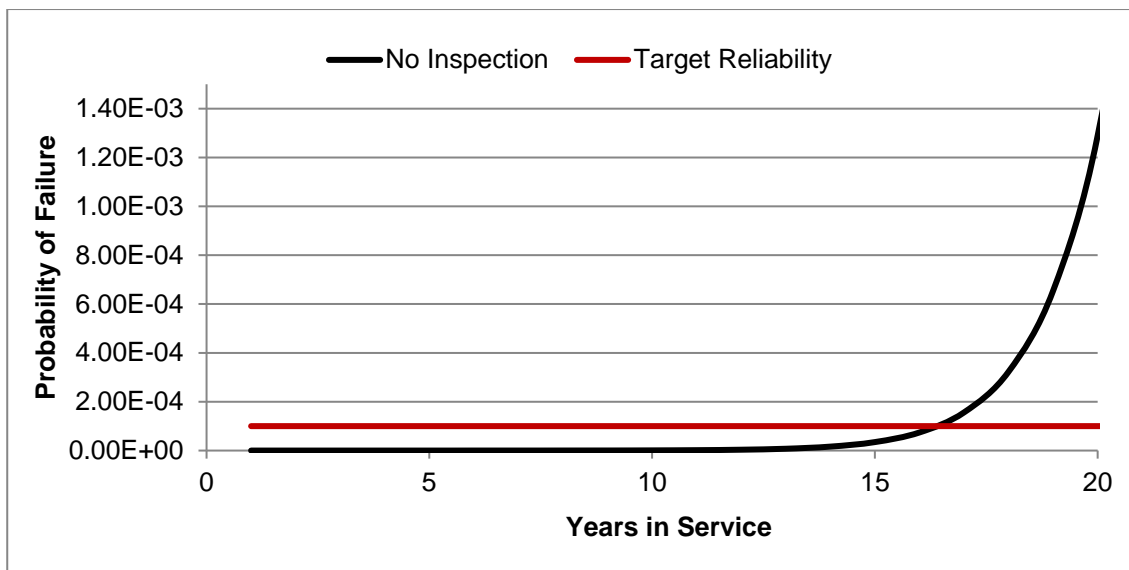


Figure 19 Example of a time-dependent fatigue and fracture reliability curve

Target reliability levels

Target reliability values may be employed to ensure that a required level of safety is achieved. The target reliability measures depend on the failure consequence as well as the cost and effort to reduce the risk of failure. The consequence of failure can be the risk of human injury and fatality, economic consequence, and social impacts. The target reliability should always correspond to a reference period, e.g. annual or service life probability of failure. If the relevant consequence is the risk of human life, annual failure probabilities are preferred to ensure a consistent level of tolerable risks at any time. Target reliabilities maybe defined four different ways:

1. The standard developers recommend a reasonable value. This method is used for novel structures.
2. Reliability implied by standards. The level of risk is estimated for a design standard that is considered to be satisfactory. This method has been commonly used for standard revisions, particularly where the intention has been to provide a more uniform safety level for different structural types and loading types. By carrying out a reliability analysis of the structure satisfying a specific code using a given probabilistic model, the implicit required level in this code will be obtained, which may be applied as the target reliability level. The advantage with this approach compared to applying a predefined reliability level is that the same probabilistic approach is applied in the definition of the inherent reliability of the code specified structure and the considered structure, reducing the influence of the applied uncertainty modelling in the determination of the target reliability level.
3. The target level for risk assessment based on failure experiences. This method is particularly useful when the functional reliability of the system is more important than the reliability of individual components. In the automotive industry or electronic components manufacturing

component reliability is determined by failure rate data of real components. The failure rate data is then used in system reliability calculation (Bertsche, 2008).

4. Economic value analysis (cost-benefit analysis). Target reliabilities are chosen to minimise total expected costs over the service life of the structure. In theory, this would be the preferred method, but it is often impractical because of the data requirements for the model. Examples of target reliabilities prescribed by codes and standards are listed in Table 6. For further information about available models for developing target reliability levels for novel structures reference is made to (Bhattacharya et al., 2001).

	Scope	Limit state function	Minimum Reliability index	Maximum Probability of failure
Euro code. Basis of structural design (BSI, 2005)	buildings and civil engineering works	Ultimate limit states (ULS)	3.3 to 4.3 for 50 years reference period and 4.2 to 5.2 for annual	4.83×10^{-4} to 8.54×10^{-6} for 50 years reference period and 1.33×10^{-5} to 9.96×10^{-8} for annual
	Residential and office buildings, public buildings where consequences of failure are medium (e.g. an office building)	Fatigue limit state (FLS)	1.5 to 3.8 for 50 years reference period	6.68×10^{-2} to 7.23×10^{-5} for 50 years reference period
DNV (DNV, 1992)	Marine structures		3.09 to 4.75	1.00×10^{-3} to 1.02×10^{-6}
IEC61400-1	Offshore Wind Turbines	ULS & FLS	3.3	5.00×10^{-4}
DNV_OS_J101	Offshore Wind Turbines (unmanned structures)	ULS		1.00×10^{-4}
DNV_OS_J101	Offshore Wind Turbines (manned structures)	ULS		1.00×10^{-5}

Table 6 Examples of target levels of reliabilities specified by standards

Application to a plate failure

Many structure members in offshore and ship shaped structure can tolerate cracks even after they become through thickness. These structure may be idealised by plates containing through thickness cracks (Figure 20).

Here, application of probabilistic fracture mechanics to such a structure is demonstrated. The assumed inputs are listed in Table 7.

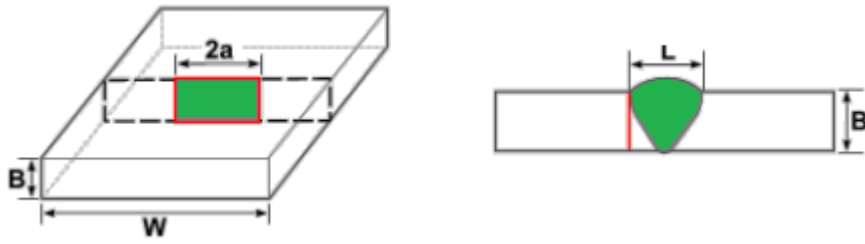


Figure 20 Through-thickness Crack geometry diagram

Case Description		
Case study structure	Offshore topside Platform with Long-term stress shape parameter = 0.85 and load cycle rate = 5.063 cycles/ min	
	Maximum design stress = 0.62 * Yield stress	
Material Properties	Young Modulus	210 constant
	Poisson Ratio	0.3 constant
	Yield stress (Y_S)	450 constant
	Tensile strength	560 constant
	Toughness	200 MPa* m ^{0.5} assumed
Fatigue assumptions	Crack growth model	Single slope Crack growth
	Cyclic stress	Equivalent constant amplitude stress 21 MPa
	Stress Intensity Solution	Through-thickness flaw in an infinite Plate
	Paris Law parameters	BS 7910 recommended values
	Design cycles in life	$N_{life} = \text{load cycle rate} \left(\frac{\text{cycles}}{\text{min}} \right) * (20 [\text{year}] * 365 [\text{day per year}] * [\text{hour per year}] * 60 [\text{min per hour}])$, for this structure = $5.322 * 10^7$
Fracture assumptions	FAD	BS 7910 Option 1
	Primary stress	Weibull distribution with scale parameter 9.47 MPa
	Secondary stress	Weld Residual stress= Constant 100 MPa, assumed
	Thickness (B)	60 (mm)
	Initial Flaw dimensions (2a)	Exponential distribution with mean value of 2 mm
Inspection Capabilities	In-service surface inspection	Surface inspection for ground welds above water surface (Figure 10)

Table 7 Inputs for probabilistic Fatigue and fracture mechanics assessment

Figure 21 shows fatigue and fracture reliability of the structure under three levels of equivalent constant amplitude cyclic stress. As a starting point, 21 MPa cyclic stress which corresponds to extreme stress of $0.62 Y_S$ is selected. Target reliability level of 1.00×10^{-4} from Table 6 for Offshore Wind Turbines (unmanned structures) is selected. The structure will reach to the target tolerable probability of failure just before year 17, suggesting that the structure should be inspected before this time. As it is shown in Figure 25, such an inspection will reduce the failure probability below the target level for the rest of the intended service life.

If the aim was to design the structure to safe-life design philosophy, the stress would have needed to be reduced below current level. This, however, would not be an economical option since the current extreme stress level already possesses significant safety factor ($0.62 Y_S$) and

reducing the stress will require bigger cross sectional dimensions and hence heavier and more expensive structure. Integrating in-service inspection options in design can potentially result in a more efficient design.

Furthermore, the design cyclic stress may be increased considering the availability of in-service inspection. Two stress levels are considered here: An upper bound limit value of 35 MPa corresponding to extreme stress equal to the Yield stress and a moderate value of 26 MPa. As depicted in Figure 21, the probability of failure curve will be shifted to left 2 and 3 years, respectively. It is evident that the structure can sustain higher levels of stresses provided that appropriate time for inspection is determined and other required limit states are not violated.

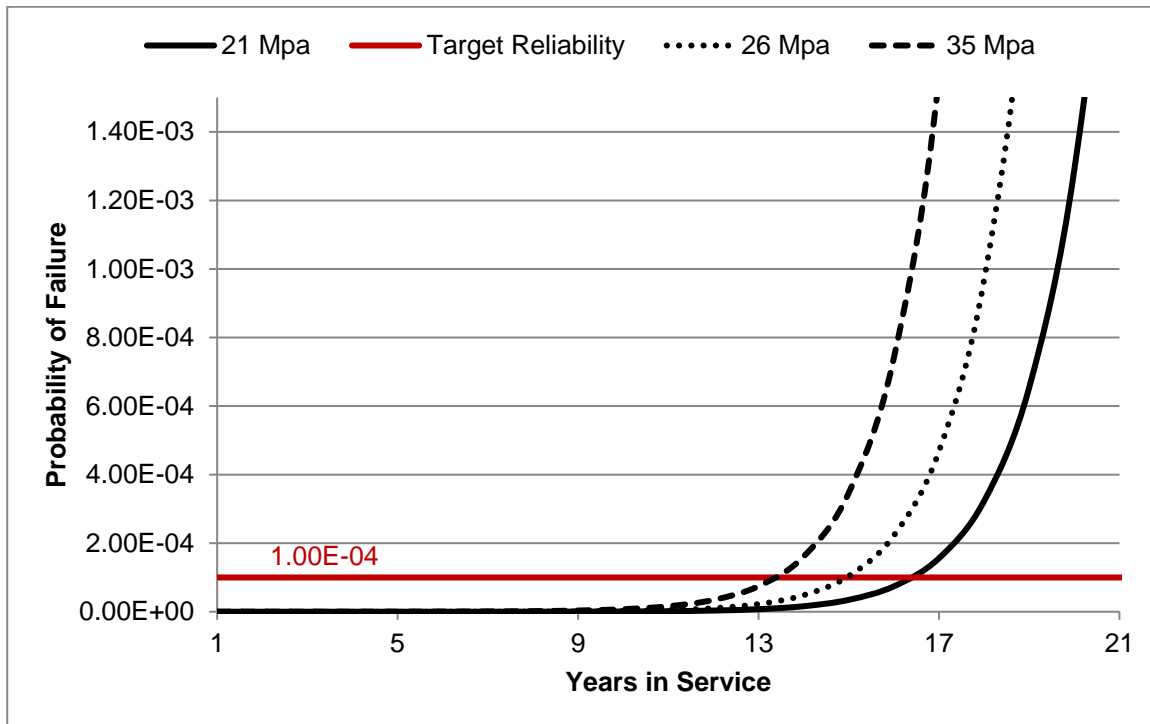


Figure 21 Fatigue reliability (FM) of a welded joint in an offshore structure for three different constant amplitude stresses

Risk Based design

The purpose of risk analysis is to comprehend the nature of risk and its characteristics including, where appropriate, the level of risk. Risk analysis involves a detailed consideration of uncertainties, risk sources, consequences, likelihood, events, scenarios, controls and their effectiveness. An event can have multiple causes and consequences and can affect multiple objectives (ISO-31000, 2018). Risk remaining after protective measures are taken is called residual risk (ISO-14971, 2012). The purpose of risk evaluation is to support decisions. Risk evaluation involves comparing the results of the risk analysis with the established risk criteria to determine where additional action is required (ISO-31000, 2018). The overall procedure for risk analysis and risk evaluation is a risk assessment (ISO-31000, 2018).

A commonly used method of risk evaluation is the so-called Risk Matrix model in which the failure probability is shown in one axis and the consequence of failure on the other. The failure probability and consequence failure maybe specified quantitatively, qualitatively, or semi-quantitatively, depending on the complexity of the model and the availability of data. Each

combination of failure probability and consequence of failure will then be assigned a corresponding risk level. It is useful to show these levels in specific colour coding convention. One such convention is an adapted traffic light convention in which low-risk levels are shown in green, extreme risks in red and medium risk levels are coloured in yellow. It is also possible to refine this colour coding further, for example, light yellow and dark yellow, to allow for more risk levels. An example Risk Matrix is shown in Figure 22.

Probability of failure	5. Frequent	HIGH	HIGH	EXTREME	EXTREME	EXTREME
	4. Likely	MEDIUM	HIGH	HIGH	EXTREME	EXTREME
	3. Possible	MEDIUM	MEDIUM	HIGH	HIGH	EXTREME
	2. Unlikely	LOW	MEDIUM	MEDIUM	HIGH	HIGH
	1. Rare	LOW	LOW	MEDIUM	HIGH	HIGH
		1. Negligible	2. Minor	3. Moderate	4. Major	5. Catastrophic
		Consequence of failure				

Figure 22 A typical Risk matrix diagram

In order to assign an appropriate risk level (i.e. colour in the risk matrix) it is necessary to establish risk acceptance levels. If a system has a risk value above the accepted levels, actions should be taken to improve the safety through risk reduction measures. One challenge in this practice is defining acceptable safety levels for activities, industries, structures, etc. Since the acceptance of risk depends upon society perceptions, the acceptance criteria do not depend on the risk value alone (Ayyub et al., 2002).

Another common risk evaluation method is the ALARP, which stands for "as low as reasonably practicable", or ALARA (as low as reasonably achievable) (HSE, 2001). The ALARP basis is that tolerable residual risk is reduced as far as reasonably practicable. For a risk to be ALARP, the cost in reducing the risk further would be grossly disproportionate to the benefit gained. The basis of ALARP is illustrated by the so-called carrot diagram in Figure 23.

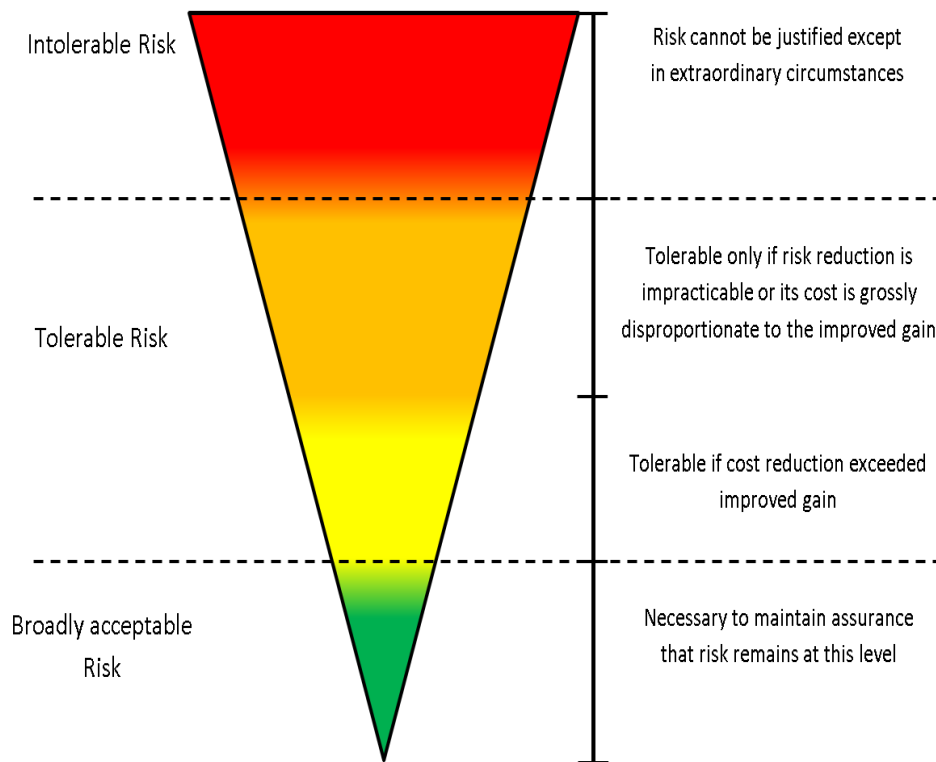


Figure 23 ALARP Carrot diagram based on (HSE, 2001)

By adopting a risk based approach in fracture mechanics for a chosen design parameter the structural design may be assessed against the corresponding risk. As an example, the design stress levels for a particular initial crack size will be associated with the corresponding risk levels, as schematised in Figure 24.

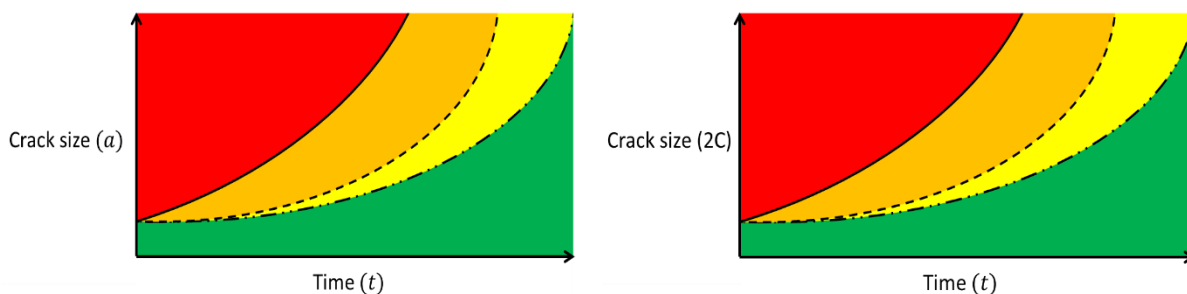


Figure 24 schematics of Crack growth curves based risk profile

Optimising inspection for design

Going back to the previous case study and as shown in Figure 25, the effect of an inspection schedule is considered for the case of through-thickness crack under 21 MPa cyclic stress. It was shown previously in Figure 21 that, the structure is predicted to reach the target tolerable probability of failure just before year 17, thus, the inspection should be scheduled prior to this time. Here, a number of inspection options are considered.

Any inspection earlier than year 6 appears to have little benefit as the failure probabilities are below $5.0\text{E-}8$, a very low probability of failure. The reduction in probability of failure is in the order of one and the structure is likely to exceed the target level of reliability again close to the final year of service. Inspection between year 10 to 15 show the most effective results by keeping the structure way below the target level throughout and to the end of service life ensuring

considerable level of safety as well as providing further life extension possibilities in the final years of designed service life.

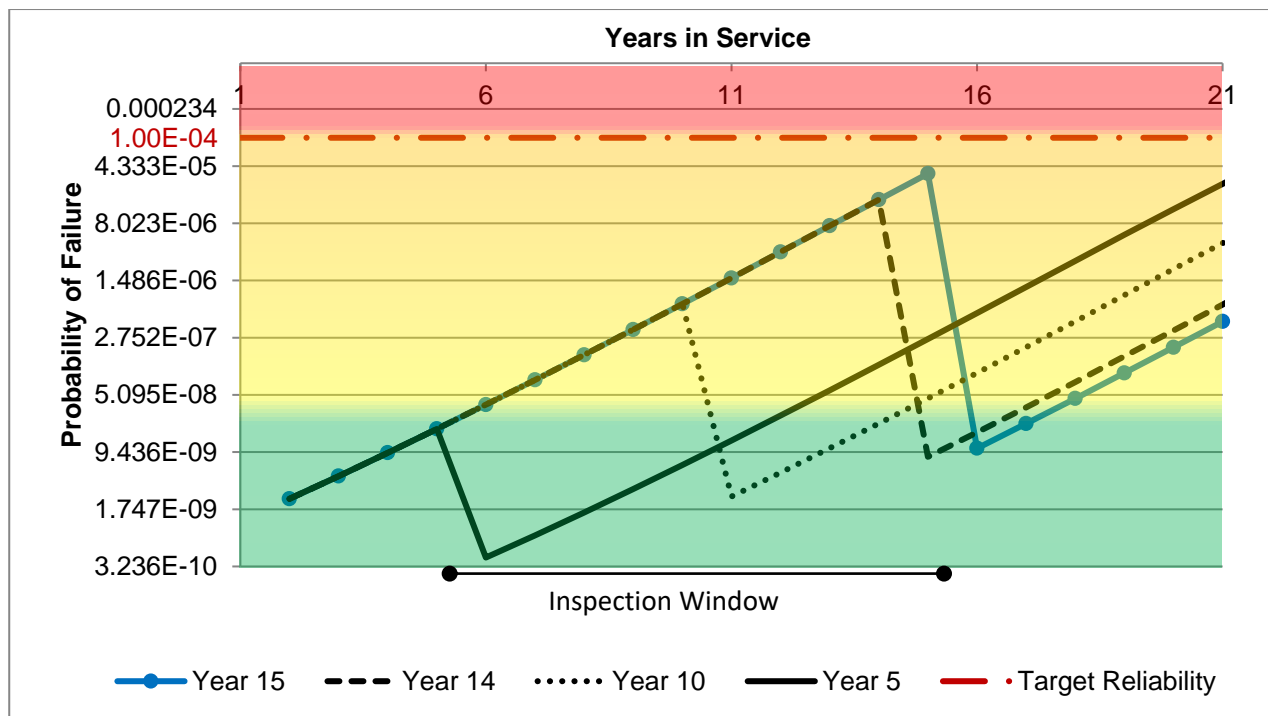


Figure 25 Crack growth curves of case study through thickness in a plate considering different first inspection times

Summary

Traditionally, design of offshore renewable structures against fatigue failure has been performed using the so-called S-N curve method. This approach, however, suffers from a number of limitations, such as limited ability to integrate the inspection capabilities. The structural design can significantly benefit from inspectability of the structure by considering the damage-tolerant nature of many offshore structures. Fracture mechanics is a powerful tool capable of address a wide range limitations associated with of the S-N approach.

In this work, a framework for design of offshore structures based on fracture mechanics was developed and its applications to a monopile wind turbine support structure were demonstrated. Additionally, probabilistic fracture mechanics approach and its application in optimising in-service NDT inspection for a plated structure under see wave loading was presented.

References

- Amirafshari, P., 2019: *Optimising Non-destructive Examination of newbuilding ship hull structures by developing a data-centric risk and reliability framework based on fracture mechanics*.
- Amirafshari, P.; Stacey, A., 2019: Review Of Available Probabilistic Models Of The Crack Growth Parameters In The Paris Equation. *OMAE2019-961*. OMAE.
- Anderson, T. L., 2005: *Fracture Mechanics: Fundamentals and Applications*.
- Ayyub, B.; Akpan, U.; Rushton, P.; Koko, T.; Ross, J.; Lua, J., 2002: *Risk-informed inspection of marine vessels*. SSC-421, Ship Structures Committee, Washington DC.

Bertsche, B., 2008: *Reliability in automotive and mechanical engineering: determination of component and system reliability*. Springer Science & Business Media.

Bhattacharya, B.; Basu, R.; Ma, K. tung, 2001: Developing target reliability for novel structures: the case of the Mobile Offshore Base. *Marine structures.*, **14**, 37–58.

BS7910, B. S., 2015: BS 7910:2013+A1:2015. *British Standards Institutions, London.*, **2015**.

BSI, 2005: BS EN 1990: 2002+ A1: 2005-Basis of Structural Design.

DNV, 1992: *Structural reliability analysis of marine structures*. Det Norske Veritas.

DNV, 2010: Fatigue design of offshore steel structures. *DNV Recommended Practice DNV-RP-C203*.

DNV, 2013: Design of offshore wind turbine structures. *DET NOR SKE VERITAS*.

DNV, 2015: *DNVGL-RP-C210-Probabilistic methods for planning of inspection for fatigue cracks in offshore structures*.

DNVGL, 2016a: DNVGL-ST-0126: Support Structures for Wind Turbines. *Oslo, Norway: DNV*.

DNVGL, 2016b: *DNVGL-ST-0437 Loads and site conditions for wind turbines*.

Gentils, T.; Wang, L.; Kolios, A., 2017: Integrated structural optimisation of offshore wind turbine support structures based on finite element analysis and genetic algorithm. *Applied energy.*, **199**, 187–204.

Georgiou, G. A., 2006: Probability of Detection (POD) curves: derivation, applications and limitations. *Jacobi Consulting Limited Health and Safety Executive Research Report.*, **454**.

HSE, 2001: *HSE's decision-making process. The Tolerability of Risk*. HSE.

IEC, 2009: 61400-3 (2009) Wind Turbines—Part 3: Design Requirements for Offshore Wind Turbines.

IEC, 2019: BS EN IEC 61400-1: Wind turbines part 1: Design requirements. *International Electrotechnical Commission*.

ISO-14971, 2012: BS EN ISO 14971: 2012—Application of risk management to medical devices.

ISO-31000, B., 2018: 31000,(2018) Risk management-Principles and guidelines. *International Organization for Standardization, Geneva, Switzerland*.

Lotsberg, I.; Sigurdsson, G.; Fjeldstad, A.; Moan, T., 2016: Probabilistic methods for planning of inspection for fatigue cracks in offshore structures. *Marine Structures.*, **46**, 167–192.

Mehmanparast, A.; Brennan, F.; Tavares, I., 2017: Fatigue crack growth rates for offshore wind monopile weldments in air and seawater: SLIC inter-laboratory test results. *Materials & Design.*, **114**, 494–504.

Naess, A., 1985: *Fatigue handbook: offshore steel structures*.

Yates, J., 2010: *Failure Assessment Diagram*. University of Manchester.